3 8006 10058 4211

CoA Memo. No. 131

August, 1967

COLLEGE OF AERONAUTICS LIBRARY

THE COLLEGE OF AERONAUTICS

DEPARTMENT OF MATERIALS

The analysis of the current shape in the circuit analogous to the a.c. welding circuit

- by -

Richard Kuszleyko

SUMMARY

The suitability for welding of manual metal arc welding transformers depends on the no-load voltage and on the electro-magnetic behaviour of the reactor. The latter is related to the curvature of the actual magnetization characteristic. The analysis aims at the quantitative establishment of that dependency.

The fulfilling of the imposed task is performed through the approximate evaluation of the current waveforms in the two simplified welding circuits that have been designed with equal parameters except the data of the reactors. The reactors have diverse magnetic circuits and when altering the two extreme working duties of the transformers, a distinctive difference arises between both the changes (for both reactors) of the magnetization characteristic curvature. The evaluation is done with a specially elaborated numerical method. When considering the results the two transformers with nearly the same proportions of the current shape at one working duty, appear to have entirely different proportions at the other working duty.

The author is with the Institute of Welding, Gliwice, Poland. In the winter and spring terms, 1967, he was an United Nations Fellow at the College of Aeronautics.

CONTENTS

1. THE ANALYSIS REASONS

The main subject

This work contributes to investigations carried out for establishing a criterion of the suitability for welding of manual metal arc welding transformers. The problem lies in selecting the primary dynamic characteristics that are required.

At present the only common method of assessing the suitability of a welding transformer is by collecting the subjective opinions of skilled welders. No physical quantities have been officially defined which can be generally used to obtain a quantitative assessment of welding transformers and to enable their comparison.

This difficulty in characterising the suitability for welding of a transformer causes confusion in the minds of purchasers and restricts the rate of development of welding power sources. Hence, a number of research centres are concerned about this problem.

The basic circuit and electro-magnetic effects

The theoretical basis for fixing the required welding suitability arises clearly from the analysis of the electrical and magnetic effects in the fundamental circuit shown in Fig. 1. This is a simplified welding circuit where less important details are neglected and the controlling inductance is represented by a single choke carrying the flux linkage ψ. U_e represents the source voltage, U_a the arc voltage and U_ψ the voltage loss in the reactor.

These quantities are related by the equation

$$U_e = U_a + \frac{d\psi}{dt} \qquad (1a)$$

Since ψ is a function of current:

$$U_e = I.R + \frac{d\psi}{dI} \cdot \frac{dI}{dt} \qquad (1)$$

R is a function of a number of variables, discussed later, and forms a time-varying resistance. The magnitude of this function determines the stability of the arc welding process. The smaller the share of the recurrent deviations of R above a mean in the total plot, then the smaller is the probability of disturbances in the welding process, which are connected with rapid changes in R induced by accidental interferences. And the smaller this share, the quieter is the welding operation. The variation of the function R reflects ionization conditions in the arc gap. It can be expressed as depending on three basic arguments:

R_s ≙ ionization influence of the medium

I ≙ arc current

$U_a = I.R$ ≙ arc voltage

i.e. $R = f_1(R_s, I, U_a)$ (2)

The term 'ionization influence of the medium' covers the influence of the whole range of quantities except the potential and the current.

The highest periodic values of the function R occur in the time period around the moment when current is passing through zero. This is due to the well known fact that in this time period the ionization of the arc gap passes through a minimum, so that there is a greater susceptibility to accidental interferences. The actual arc gap voltage is of great importance at that moment.

The principles of comparison of the dynamic properties

From the point of view of a welding power source there are two possibilities for the modelling of the solution of the basic circuit equations. Thus there are two possible ways to the correction of the waveforms I, $U_a = I.R$ and of the examined actual rates of R, according to the relationship (2). In equation (1) these two possibilities correspond to the changing of the terms U_e and $\frac{d\psi}{dI}$, whereas in practice they mean a selection of the supply voltage (or no-load voltage) and of the 'inductance action form'. Generally speaking, in basic circuit equations (which may include simultaneous equations instead of a single equation (1)) 'inductance action form' corresponds to terms connected with internal relationships of the controlling inductance. In the case of a circuit such as shown in Fig. 1 this form results directly from the selection of the family of characteristics $\psi = f(I)$ (which typify the magnetization curve) for the reactor.

Both the above aspects must be reflected in any criterion of the suitability for welding. They were considered in the literature, such as references 1, 2 and 3.

The most rational way to compare the suitability for welding of various transformers would involve the determination of the R values resulting (for various transformers) from the identical functional dependences f_1 at the identical medium-ionization-influences R_s. Such a way, however, seems to be impracticable at present, so the only possible quick method that remains is the consideration of both the above mentioned causes (i.e. supply voltage and inductance action form) that, as far as the power source is concerned, determine the operation of the process.

The U_e comparison does not present great practical difficulties since it can be carried out as a comparison of the rms no-load voltage. However, the estimation of the inductance action form, on the contrary, requires a more complicated procedure. The most plastic and best although not entirely adequate method for this appears to be through the comparison of the shapes of the currents flowing throughout a circuit at special, conventional conditions. A major problem of the method lies in defining these conditions.

The inductance action form is tied to the character of the function $\frac{d\psi}{dI}$ in a given configuration. This character depends on the initial conditions determined by the control settings of the transformer, and on the actual current peaks. In the case of the ideal test method described above (at a given relationship f_1, given R_s) performed for a given welding process, it would be possible to meet satisfactorily such dependences merely by the qualitative and quantitative defining of the current value and by experimental adjustment of the transformer controls according to these data.

Of all the parameters which may be used to define a periodic function, that most applicable to weld current is the root mean square value. This is significant in the welding process analysis, and therefore should be used as a basic argument in the discussed estimation. Nevertheless, if the rms value is used, the real $\frac{d\psi}{dI}$ transition range for a given rms current value, and the once determined coefficient of the current shape at this rms value, correspond precisely one to the other only for the original transformer control settings and for the original f_1 and R_s values. If, however, the maximum value were used, the real $\frac{d\psi}{dI}$ transition range for a given maximum current value, and the once obtained coefficient of the current shape at this maximum value, would correspond precisely one to the other for the original transformer control settings as the only restriction.

As an approximation for practical purposes, the ideal test method may be replaced by a comparison of the current shapes at the identical nominal settings of the controllers, i.e. settings that provide a given rms current value in the circuit when the arc is replaced by a linear resistance calculated as a quotient of conventional load voltage and rms current value. Such a nominal setting and such a linear resistance give two conditions that are necessary and sufficient for the discussed practical comparison of the current shapes. One of the two constituents of practical evaluation of the suitability for welding can thus be determined.

Carrer's method

The evaluation of both the above factors (no-load voltage and current shape) provides a basis for the most common practicable method of defining the suitability for welding of transformers. The method was elaborated by Professor Antonio Carrer[1,2]. As a current shape factor, he applied a reduced tangent of the angle that was enclosed between the time axis and the graph of the current wave in the period after passing through zero, that is in the period that carries the greatest probability of the initiation of a disturbance.

The above mentioned conversion feature that is most essential from the point of view of the considerations presented in this paper, is a division of that tangent when divisor composed as the maximum current value. Reduced tangent and rms no-load voltage form a coefficient which is indicative of the suitability for welding of the transformer.

All the theoretical considerations, which were briefly mentioned earlier, confirm the soundness of the principles of Carrer's method if the current shape factor is connected with one given work current value. However, in the delineation of the method there is no substantial restriction defining accurately that it is insufficient to characterize the total (between ultimate adjustments) duty range of transformer when using only one figure, derived in the proposed way. The $\psi = f(I)$ curvature may undergo large changes with variations in the controller adjustment. Radical alterations may then occur in the current shape proportions, relating as well to the quotient of considered tangent and maximum current value. It must be stressed that the figure is valid only for the regime approaching the one for which the coefficient was determined. A single current shape factor could give an improper indication of the transformer suitability, particularly when the transformers under comparison have diverse regulating ranges.

The task of the analysis

Although in the theory it is evident that proportions of the current shape depend on the $\psi = f(I)$ curvature, still for practical purposes the quantitative scrutiny of this relation is necessary. Such an investigation is realised in the present work. It aims to evaluate a few characteristic waveforms of current in a simplified welding circuit corresponding to the conventional linear conditions for the defining of the current shape. The waveforms relate to a few assorted $\psi = f(I)$ curvatures. The circuit is formed as in Fig. 1, but U_a is replaced by the voltage drop on the linear resistance R based on the quotient of conventional load voltage and rms current value.

For the purpose of creating convenient prerequisites for the estimation of the influence of the $\psi = f(I)$ curvature, it is resolved to evaluate the waveforms at equivalent working duties in the two circuits with specially selected parameters as explained below.

The equivalent duties here refer to the duties at the same maximum current value, for both circuits. Such a promise facilitates the analysis and increases clarity of the results. The approximate equalization is performed by the adjustment of the transformer controllers. The 3% difference in the equivalent (maximum) current values has been admitted.

Two working duties are taken into consideration:

'O' - low current range
'K' - high current range.

The considered circuits are supposed to have:

(a) Identical constant sinusoidal voltages U_e
(b) Identical linear resistances

R_0 - at '0' duty

R_K - at 'K' duty

(c) Different changes of the curvatures of the utilised sections of the reactor saturation characteristics, when shifting the duties.

In the realization of the primary task of the analysis there are four necessary stages aiming to:

(a) The elaboration of the evaluation method.
(b) The design of the reactors and of the electrical circuit parameters.
(c) The evaluation of the magnetic characteristics.
(d) The calculation and the plotting of the results.

2. THE EVALUATION METHOD

When assuming that U_a is replaced by the product of current and linear resistance R, then equation (1a) becomes

$$U_e = I.R + \frac{d\psi}{dt}$$

Since $\psi = w.\Phi$

where $\Phi \equiv$ magnetic flux in the choke

$w \equiv$ number of turns

then

$$U_e = I.R + w\frac{d\Phi}{dt} \qquad (3)$$

or:

$$\frac{U_e}{w.Q} = \frac{dB}{dt} + H.R.\frac{1}{w^2.Q}$$

where $B \equiv$ magnetic flux density

$H \equiv$ magnetic field strength

$Q \equiv$ effective core area

$l \equiv$ mean flux path

If

$$\frac{U_e}{w.Q} = \ddot{U}_e \text{ and } R.\frac{1}{w^2.Q} = \ddot{R} \qquad (4\ a,b)$$

then

$$\ddot{U}_e = \frac{dB}{dt} + H.\ddot{R}$$

The magnetization curve gives the relationship

$$B = f_B(H) \qquad (5)$$

Referring to this,

$$\ddot{U}_e = \frac{dB}{dH} \cdot \frac{dH}{dt} + H.\ddot{R}$$

and

$$\frac{dH}{dt} = \frac{\ddot{U}_e - H.\ddot{R}}{\frac{dB}{dH}} \qquad (6)$$

This equation should be integrated when:

(a) Knowing the function $\ddot{U}_e$, that is, when $\ddot{U}_e$ can be evaluated for all the time-values from the considered interval, and

(b) knowing the function $\frac{dB}{dH}$, that is, when $\frac{dB}{dH}$ can be evaluated for all the H values from the considered set. Hence if the value of H is known for a given instant, then the $\frac{dB}{dH}$ value can also be evaluated for that instant.

The relationship from (5), which determines the $\frac{dB}{dH}$ function, is normally given as a table that cannot be expressed in a simple mathematical formula. For the purpose of the evaluation of the actual current shape in the circuit with ordinary choke, it cannot be even approximated by a simple relationship, as it is often applied in the magnetic amplifier analysis. Thus, the only way to integrate equation (6) is by using a numerical method. In this work an original one was developed, on the basis of the Heun's (improved Euler) method.[4]

If the differentials dH and dt are substituted by finite increments, then equation (6) becomes

$$H(t_{m+1}) - H(t_m) = \frac{\ddot{U}_e(t_m) - \ddot{R}.H(t_m)}{\left(\frac{dB}{dH}\right)(t_m)} \quad (t_{m+1} - t_m) \qquad (7)$$

where t_m and t_{m+1} denote two instants adjacent in the considered sequence.

The method carries a premise that $H(t_m)$ is known, i.e. that the value of the function H has been evaluated for any instant. This makes a starting point for the next evaluation:

$$H^*(t_{m+1}) = H(t_m) + \frac{\ddot{U}_e(t_m) - \ddot{R}.H(t_m)}{\left(\frac{dB}{dH}\right)_{(t_{m+1})}} \cdot (t_{m+1} - t_m) \qquad (8)$$

and then, analogously:

$$H^*(t_{m+2}) - H^*(t_{m+1}) = \frac{\ddot{U}_e(t_{m+1}) - \ddot{R}.H^*(t_{m+1})}{\left(\frac{dB}{dH}\right)^*_{(t_{m+1})}} \cdot (t_{m+2} - t_{m+1}) \qquad (9)$$

The characters * denote the auxiliary values - representing a first iteration.

The desired value $H(t_{m+1})$ is evaluated from a formula based on the mean of the two H slopes that correspond to the points $H(t_m)$ and $H^*(t_{m+1})$:

$$H(t_{m+1}) = H(t_m) + (t_{m+1} - t_m) \cdot \frac{1}{2}\left[\frac{H^*(t_{m+1}) - H(t_m)}{t_{m+1} - t_m} + \frac{H^*(t_{m+2}) - H^*(t_{m+1})}{t_{m+2} - t_{m+1}}\right]$$

If $(t_{m+1} - t_m) = (t_{m+2} - t_{m+1})$

then

$$H(t_{m+1}) = H(t_m) + \frac{[H^*(t_{m+1}) - H(t_m)] + [H^*(t_{m+2}) - H^*(t_{m+1})]}{2} \qquad (10)$$

Formulae (8), (9) and (10) define the operations for the successive evaluating of H for all the considered instants. Conversion of H into the current can be performed by a simple multiplication according to the formula

$$I = H \cdot \frac{1}{w} \qquad (11)$$

Obviously, these formulae can be applied practically only in the case when the initial conditions have been defined. Hence it must be known what is the value of H for the first considered instant. In this work this problem has been solved in the following way:

(a) For the initial instant (t=0) it is assumed that H = 0 and, therefore, $\Phi = 0$.

(b) The appropriate phase angle of the supply voltage is selected. Referring to the general relationship for sinusoidal waveform,

$$U_e = \underline{U_e} \cdot \sin(\omega.t + \rho)$$

where $\underline{U_e}$ = maximum voltage value.

For the moment when H, as well as Φ, pass through the maximum value, equation (3) becomes

$$\underline{U_e}.\sin(\omega.t_{max} + \rho) = \underline{I} \cdot R$$

where $\underline{I}$ = maximum current value

hence

$$\sin(\omega.t_{max} + \rho) = \frac{\underline{I} \cdot R}{\underline{U_e}}$$

Approximately

$$\omega.t_{max} = \pi$$

so

$$\cos \rho = \frac{\underline{I}.R}{\underline{U_e}} \qquad (12)$$

In this way, the evaluated current waveforms begin always from zero, but each working duty is accompanied by a particular phase angle of the supply voltage.

3. THE ELECTRICAL CIRCUIT PARAMETERS AND THE REACTOR

The two considered working duties are resolved as '0' working duty - at the 50A maximum current value range, and 'K' working duty - at the 300A maximum current value range. This corresponds to the common regulating ranges in welding transformers of medium size.

The no-load constant sinusoidal voltage is 70V for both considered circuits and both duties.

The linear resistance is evaluated according to the Polish standards that determine the conventional load voltage as:

$$u_a = 20 + 0.04.i \qquad (13)$$

where $u_a \equiv$ rms voltage, in volts

$i \equiv$ rms welding current, in amperes.

This corresponds approximately to other welding standards as well.

Substituting symbols by actual values and (exceptionally, for this aim only) applying a relationship for sinusoidal waveforms:

$$u_{a0} = 20 + 0.04 \quad \frac{50}{\sqrt{2}} = 21.4 \text{ V}$$

$$u_{aK} = 20 + 0.04 \quad \frac{300}{\sqrt{2}} = 28.5 \text{ V}$$

From that the resistances:

$$R_0^* = \frac{21.4.\sqrt{2}}{50} = 0.606\ \Omega$$

$$R_K^* = \frac{28.5.\sqrt{2}}{300} = 0.134\ \Omega$$

When about 0.025Ω is added for usual circuit resistance, the desired values of R become

$$R_0 = 0.63\Omega \qquad R_K = 0.16\Omega \qquad \text{(for both circuits)}$$

The two chokes A and B, for the two considered circuits, are designed on the same construction principle, with the variable air gap concept. The projected chief parameters are shown in Fig. 2. They differ considerably since it is intended to provide convenient opportunities for the comparison. The lamination factor is assumed as 0.92.

Referring to the above data, the evaluation of the magnetic circuit parameters proceeds as follows:

Mean length of the flux path

$$I_A = 4.(20+7) = 108 \text{ cm}$$

$$I_B = 4.(36+13) = 196 \text{ cm}$$

Effective core area

$$Q_A = 49.0.92 = 45 \text{ cm}^2$$

$$Q_B = 169.\ 0.92 = 155 \text{ cm}^2$$

Maximum field strength value for 'K' duty

$$\underline{H_{AK}} = \frac{50 \times 300}{108} = 138.8 \text{ A/cm}$$

$$\underline{H_{BK}} = \frac{20 \times 300}{196} = 30.6 \text{ A/cm}$$

If all the waves were sinusoidal, the desired voltage losses in the reactor could be calculated from the voltage-drop triangle:

(rms values)

$$70^2 = 0.63^2 \times 50^2 \left(\frac{1}{\sqrt{2}}\right)^2 + u^2_{\psi 0}$$

$$70^2 = 0.16^2 \times 300^2 \left(\frac{1}{\sqrt{2}}\right)^2 + u^2_{\psi K}$$

so that

$$u_{\psi 0} = 66.2\text{V} \qquad u_{\psi K} = 61.1\text{V}$$

In that case the maximum values of flux density for '0' duty would become:

$$\underline{B_{A0}} = \frac{66,2 \times 10^4}{4,44 \times 50 \times 50 \times 45} = 1.32 \text{ Wb/m}^2$$

$$\underline{B_{B0}} = \frac{66,2 \times 10^4}{4.44 \times 50 \times 20 \times 155} = 0.96 \text{ Wb/m}^2$$

4. THE MAGNETIZATION CHARACTERISTICS

According to a basic electrotechnical relation, the magnetic flux density in the air gap is due to the undermentioned proportionality with the magnetic field strength:

$$B_g = 4.\pi \times 10^{-5} . H^*_g \qquad (14)$$

where B_g = magnetic flux density in the air gap, in Wb/m^2

H^*_g = magnetising force (magnetic field strength) necessary along the air gap in A/cm.

Referring to Fig. 2,

$$H^*_g = \frac{\theta_g}{l_0} \qquad (15)$$

where θ_g = magnetomotive force necessary along the air gap, in A.

For practical purposes, however, it is convenient to use

$$H_g = \frac{\theta_g}{l_1} \tag{16}$$

instead of H^*_g.

From (15) and (16)

$$\frac{H_g}{H^*_g} = \frac{l_0}{l_1} = \xi \tag{17}$$

The actual area of air gap differs from the effective core area. This fact can be formulated by using a space factor ν:

$$Q_{gap}.\nu = Q$$

Hence, the density in the core

$$B = B_g.\frac{1}{\nu} \tag{18}$$

From (14), (16) and (17)

$$\frac{B}{H_g} = \frac{1}{\nu} \cdot \frac{l_1}{l_0} \cdot 4.\pi.10^{-8}$$

In the present work it is assumed that $\nu = 1$. This assumption does not affect any final results of the analysis, since the selection of ξ could be supposed as the selection of the product

$$\nu \cdot \frac{l_0}{l_1}.$$

If $\nu = 1$ then $B = B_g$ and

$$H_g = B.\xi.\frac{10^8}{4.\pi} \tag{19}$$

Expression (19) describes the family of straight lines that show the converted (from H^*_g to H_g) magnetization characteristics of the air gap by various ξ valves. All lines pass through the origin of co-ordinates, thus for plotting it is sufficient to determine one point (of each line) only.

The total necessary excitation of the circuit is

$$\theta = H_g.l_1 + H_\mu.l$$

where $H_\mu \equiv$ magnetising force necessary along the iron path, in A/cm

$l \equiv$ length of the iron path, in cm.

Usually the $l_o = (l_1 - l_\mu)$ does not exceed 2% of l_1. So approximately

$$l_\mu = l_1 \tag{20}$$

and

$$H = \frac{\theta}{l_1} = H_g + H_\mu \tag{21}$$

Hence, the overall magnetization characteristic, for the total loop, results from the successive additions of the field strength values that correspond to the same density value in the gap characteristic - (19) - as well as in the fundamental magnetization characteristic, i.e. the characteristic for the loop when the air gap is eliminated ($\xi = 0$). In the presented work, this addition is performed partially as a graphical construction.

Originally, the fundamental magnetization characteristic was resolved in this work as a normal induction curve for the 300A welding choke that was based on the core constructed with the interleaved assembly of laminations. The Polish transformer plates E4 have been used. These are manufactured as high resistance non-oriented sheets; 0,35 mm nominal thickness; 1,2 W/kg power loss at 1 Wb/m^2. The curve has been estimated through the measurements of

maximum flux density - evaluated from the rms voltage induced in a special auxiliary winding,

maximum field strength - evaluated from the maximum current indications of the valve-type instrument.

The results are given in Table 1.

TABLE 1

H A/cm	B Wb/m²	H A/cm	B Wb/m²	H A/cm	B Wb/m²	H A/cm	B Wb/m²
0.00	0.00	1,38	0.61	7.8	1.08	28 6	1.36
0.27	0.01	1,58	0.66	9,4	1.12	39.8	1.43
0,35	0.02	2.05	0.74	10,9	1.15	48.1	1.47
0,43	0.05	2,82	0.83	12.4	1,18	59.2	1,51
0,54	0,07	3.43	0,88	14.4	1.21	82.0	1.57
0,63	0,11	4.03	0,92	17,1	1.25	111.6	1.62
0,96	0,44	4,69	0.96	20.7	1.29	139,6	1.65
1.06	0,50	5,30	0.99	23.7	1,32	178,0	1.67
1.20	0.56	6,05	1.02				

Fig. 3 shows the estimated component characteristics, i.e. the fundamental magnetization characteristic according to the above table, and the air gap characteristics that have been evaluated from expression (19)

for ξ = 0.125; 0,25; 0.375; 0.5; 0.75; 1; 1.25; 1.5; 2; 3 and 4.10^{-2}.

Fig. 4 presents the family of the overall magnetization characteristics that have been constructed graphically according to formula (21). On this figure it could be verified that the position of the extreme sinusoidal working points differ considerably for choke A and choke B. If all the waveforms were sinusoidal, then the points (recalling the values from chapter 3) would be located:

Choke A

$$H_{AO} = \frac{138.8}{6} = 23.1 \text{ A/cm} \qquad B_{AO} = 1.32 \text{ Wb/m}^2$$

$$H_{AK} = 138.8 \text{ A/cm} \qquad B_{AK} = 1.32 \frac{61.1}{66.2} = 1,22 \text{ Wb/m}^2$$

Choke B

$$H_{BO} = \frac{30.6}{6} = 5.1 \text{ A/cm} \qquad B_{BO} = 0.96 \text{ Wb/m}^2$$

$$H_{BK} = 30,6 \text{ A/cm} \qquad B_{BK} = 0.96 \frac{61.1}{66,2} = 0.89 \text{ Wb/m}^2$$

TABLE II (H in A/cm^2, $\frac{dB}{dH}$ in $\frac{Wb/m^2}{A/cm}$ $.10^{-3}$

$\xi = 0$		$0{,}125\ 10^{-2}$		$0.25\ 10^{-2}$		$0.375\ 10^{-2}$		$1{,}25\ 10^{-2}$		$1.5\ 10^{-2}$	
H	$\frac{dB}{dH}$	H	$\frac{dB}{dH}$	H	$\frac{dB}{dH}$	H	$\frac{dB}{dH}$	H	$\frac{dB}{dH}$	H	$\frac{dB}{dH}$
0.1	37	0.2	27	0,2	21.3	0.3	17.6	0.6	7.9	0,7	6,83
0,3	125	0,5	55.6	0,6	35.7	0,8	26.4	1,8	9.3	2.1	7,84
0.4	231	0.8	69.8	1.1	41.2	1.5	29.2	3.9	9.64	4.6	8.09
0.5	333	1.1	77	1.6	43.8	2.3	30.5	6.5	9.77	7.7	8.17
0.6	444	1,5	81.7	2.3	45.1	3.3	31.1	9.5	9.85	11.4	8,23
0.8	1000	3.0	91,1	6,2	47.8	9.0	32.5	28.1	9,98	33.7	8,31
1.0	600	5,7	85.8	10.3	46.2	15,0	31.7	47.8	9,89	57,3	8.27
1.1	428	6.4	81	11.7	49.9	16.9	31.1	53.9	9.82	64.5	8.22
1,3	277	7.1	73.6	13.0	42.5	18,7	29.9	59.5	9,7	71.2	8,13
1,5	250	7,8	71,3	14.1	41.8	20.4	29.6	64.7	9,65	77.4	8.11
1,8	170	8.8	63	15.7	38.9	22.2	28.1	71,5	9,48	85,4	8
2.4	117	10.3	54	18,0	35.2	25.9	26.1	80,5	9.25	96.1	7.82
3.1	82	11.7	45.1	20.1	31,1	28.6	23.8	88.1	8,94	105.3	7.6
3.7	66.8	12,7	40	21.6	28.7	30,5	22.4	93.1	8.73	111.3	7.44
4.4	60,6	13.8	37.7	23.1	27.5	32,4	21.6	97.8	8.6	116.8	7.34
5.0	49.1	14.7	33	24,4	24.8	34.0	19.92	101,9	8.35	121.5	7.18
5,7	40	15,7	28,6	25.7	22.3	35.7	18.25	105.5	8.03	125.7	6.9
6,9	34,2	17,3	25.5	27,8	20.3	38.3	16.9	111,3	7,76	132.4	6.73
8.6	25	19.5	20	30,5	16.65	41.5	14.3	118,0	7,18	140.0	6.28
10.1	20	21,4	16.6	32.7	14.28	44.0	12.5	122.9	6.7	145.7	5.91
11.7	20	23,2	16.6	34,7	14,28	46.4	12.5	127,4	6.7	150.8	5.91
13,4	15	25,2	13	37,2	11.55	49.1	10.35	132.2	6.02	156.2	5.39
15.8	14.8	28.0	12,9	40,2	11.42	52 5	10.26	138.0	6.0	162.6	5.35
18.9	11.1	31.5	10	44,2	9,1	56.9	8.35	145.1	5.28	170.5	4.78
22.2	10	35,2	9.1	48,2	8.33	61.2	7,71	151,9	5,01	178.1	4.57
26.1	8.17	39.5	7.55	52,8	7,01	66.0	6,58	159.4	4.5	186,2	4.13
34.2	6.24	48,0	5,88	62,0	5.56	75.8	5.28	172,9	3.96	200.9	3,58
43.9	4.81	58.4	4,6	72,8	4.4	87.3	4.21	188.2	3,26	217,3	3.06
53.2	3.60	68,0	3.48	82.8	3.36	97,6	3,26	201.4	2.65	231.2	2.52
70.6	2.63	85.9	2.56	101,2	2.5	116.6	2,44	223.8	2.08	254.6	2
96.8	1.69	112,7	1,66	128.5	1,64	144.4	1.56	255.5	1.445	287,2	1,405
125.6	1,07	141.8	1.06	158.1	1.05	174,3	1.036	288.3	0.968	320.7	0.951
158.8	0.521	175.3	0.519	191.8	0.515	208.3	0.512	324.0	0.493	357.0	0.49

When altering the duties, the curvatures of the (utilised sections of) characteristics undergo changes that are explicitly dissimilar for choke A and choke B.

For the purpose of the discussed analysis it is necessary to adapt magnetization characteristic by converting it into a characteristic of the derivative $\frac{dB}{dH}$, which is incorporated in the formulae (8) and (9). The conversion has been performed here, approximately, by the calculation of: (a) the increments of B from Table I, (b) the increments of H, resulting from the addition of the increments calculated from Table I and the increments by using formula (19), and (c) the quotients of increments B over increments H.

The abscissae of evaluated points $\frac{dB}{dH}$ are assumed to be the arithmetic means of the H values that are calculated for both limits of the interval corresponding to the considered increment.

The $\frac{dB}{dH}$ characteristics have been evaluated for ξ = 0; 0.125; 0.25; 0.375; 1.25 and 1.5 10^{-2}. The results are presented in Table II and plotted in Figure 5.

Because of the $\frac{dB}{dH}$ peaks, the initial part of the evaluated characteristics is inconvenient for the discussed numerical analysis. Without seriously affecting the results this can be avoided when the initial part of the fundamental induction curve is substituted by a straight line reflecting an idealized mean process of magnetization. In this work it is assumed that the discussed straight line passes through the origin of the co-ordinates and through a defined point of the magnetization characteristics. The point must correspond to the same $\frac{dB}{dH}$ value as the one for the straight line approximation.

The fulfilling of this requirement at ξ = 0 has been performed through the graphical determination of the point common for:

(a) the characteristic $\frac{dB}{dH} = F(H)$ for the normal induction curve, and

(b) the characteristic $\frac{B}{H} = F_1(H)$ for this curve.

The graphs are shown in Figure 6. This gives the approximate co-ordinates of the intersection:

$$470.10^{-3} \frac{Wb/m^2}{A/cm} \quad \text{and } 1.1 \text{ A/cm}$$

The corresponding magnetic flux density is 0.518 Wb/m^2.

The modified normal induction curve is shown in Figure 7.

For other values of ξ, the points that define the limit of the $\frac{dB}{dH}$ constancy, have been evaluated according to the above data and to the formulae (19) and (21). The results of the evaluation are presented in Table III.

TABLE III. (H_s In A/cm, $\frac{dB}{dH}$ in $\frac{Wb/m^2}{A/cm} .10^{-3}$)

	$\xi = 0$	$0.125\ 10^{-2}$	$0,25\ 10^{-2}$	$0.375\ 10^{-2}$	$1,25\ 10^{-2}$	$1,5\ 10^{-2}$
H_s	1.1	6,2	11.4	16.5	52.4	62.8
$\frac{dB}{dH}$	470	83	45,3	31.3	9.85	8,25

5. THE WAVEFORMS

The evaluation of the current waveforms proceeds on the basis of formulae (8), (9) and (10). Thus at first the waveforms of the magnetic field strength are evaluated. After that, these waveforms are converted into the current waveforms, according to formula (11).

The preliminary calculation comprises the determination of the voltage function U_e and of the reduced resistance R, which corresponds to the parameters from chapter 3.

The maximum value of the voltage U_e:

$$\underline{U_e} = 70\sqrt{2} = 98.8 \text{ V}$$

According to expression (12):

at '0' duty

$$\cos \rho_0 = \frac{50 \times 0.63}{98.8} = 0,318$$

and $\rho_0 = 71°27'$

at 'K' duty

$$\cos \rho_K = \frac{300 \times 0,16}{98,8} = 0,486$$

and $\rho_K = 60°55'$

According to expression (4a):

for choke A

$$\underline{\ddot{U}_{eA}} = \frac{98,8 \times 10^4}{50.45} = 440 \text{ V/m}^2$$

for choke B

$$\ddot{\underline{U}}_{eB} = \frac{98.8\ 10^4}{20\ 155} = 318 V/m^2$$

According to expression (4b):

for choke A

$$\ddot{R}_{OA} = 0.63\ \frac{108\ 10^4}{50^2\ 45} = 6.05 \frac{\Omega.cm}{m^2}$$

$$\ddot{R}_{KA} = 0.16\ \frac{108\ 10^4}{50^2\ 45} = 1,537 \frac{\Omega.cm}{m^2}$$

for choke B

$$\ddot{R}_{OB} = 0.63\ \frac{196\ 10^4}{20^2\ 155} = 19.9\ \frac{\Omega.cm}{m^2}$$

$$\ddot{R}_{KB} = 0.16\ \frac{196\ 10^4}{20^2\ 155} = 5.07\ \frac{\Omega.cm}{m^2}$$

As it was planned, the H (and current) waveforms are evaluated for the chokes A and B at both the working duties. On account of the symmetry (of the odd-harmonic type) of the waves, half of the cycle only is taken into consideration. The time-period of this half-cycle is divided into 10 equal intervals that determine the evaluation points. If the line frequency is 50 kcps, then each of the intervals is equal to 0.001 sec. The waveforms at '0' duty are evaluated with an additional point related to 0.0045 sec. The corresponding H value is calculated as the arithmetic mean of the increments evaluated when starting from:

(a) the point 0.004 sec.
(b) the point 0.005 sec. (evaluation 'backwards').

The course of evaluation is demonstrated in Table IV. This presents the details of the calculation for the choke A at '0' duty ($\ddot{R} = 6.05$). The resolved ξ equals zero. The $\frac{dB}{dH}$ values are taken from Fig. 5 (assuming the limit of $470\ 10^{-3}\ \frac{Wb/m^2}{A/cm}$).

At 0.0045 sec:

$$H = \frac{27.9 + 21.0}{2} \simeq 24.5\ A/cm.$$

The complete results of the evaluation of H are given in Table V and plotted in Figs. 8, 9, 10 and 11.

The corresponding settings of the chokes are:

	'0' duty	'K' duty
Choke A	$\xi = 0$	$\xi = 1.25\ 10^{-2}$
Choke B	$\xi = 0$	$\xi = 0.375\ 10^{-2}$

TABLE IV (t in sec, $\ddot{U}_e$ in V/m², H in A/cm, $\ddot{R}$ in Ω.cm/m², $\frac{dB}{dH}$ in $\frac{Wb/m^2}{A/cm}$ $.10^{-3}$

t_m	$\omega.t_m + \rho$	$\sin(\omega.t_m+\rho)$	$\ddot{U}_e(t_m)$	$H(t_m)$	$\ddot{R}.H(t_m)$	$\ddot{U}_e(t_m)-\ddot{R}.H(t_m)$	$(\frac{dB}{dH})(t_m)$	$\Delta H^*(t_m)$	$H^*(t_{m+1})$	$\ddot{R}.H^*(t_{m+1})$	$\ddot{U}_e(t_{m+1})-\ddot{R}.H^*(t_{m+1})$	$(\frac{dB}{dH})^*(t_{m+1})$	$\Delta H^*(t_{m+1})$	$\Delta H(t_m) = \frac{\Delta H^*(t_m)+\Delta H^*(t_{m+1})}{2}$
0.	71°30'	0.948	418	0.0	0	418	470	0.9	0.9	5	435	470	0.9	0.9
0.001	89°30'	1.000	440	0.9	5	435	470	0.9	1.8	11	410	155	2.6	1.8
0.002	107°30'	0.954	421	2.7	16	405	93	4.4	7.1	43	316	31	10.2	7.3
0.003	125°30'	0.814	359	10.0	60	299	21.8	13.7	23.7	143	119	8.8	13.6	13.7
0.004	143°30'	0.595	262	23.7	143	119	8.8	13.6	37.3	226	86	5.55	-15.4	-0.9
0.005	161°30'	0.317	140	22.8	138	2	9.2	0.2	23.0	139	-135	9.2	-14.7	-7.3
0.006	179°30'	0.009	4	15.5	94	-90	13.8	-6.5	9.0	54	-186	24.5	-7.6	-7.1
0.007	197°30'	-0.301	-132	8.4	51	-183	26.1	-7.0	1.4	8	-264	240	-1.1	-4.1
0.008	215°30'	-0.807	-256	4.3	26	-282	52.1	-5.4	-1.1	-7	-347	470	-0.7	-3.1
0.009	233°30'	-0.948	-354	1.2	7	-361	390	-0.9	0.3	2	-420	470	-0.9	-0.9
0.01	251°30'		-418	0.3										
				23.7				6.8	30.5	184	20	6.82	1.5	4.2
0.0045	152°30'	0.762	204	27.9										
				22.8				-0.1	22.7	137	67	9.3	-3.6	-1.8
			204	21.0										

TABLE V

Time, sec.	Magnetic field strength, A/cm.			
	'O' duty		'K' duty	
	Choke A	Choke B	Choke A	Choke B
0.	0,0	0.0	0.0	0.0
0,001	0,9	0.65	38.3	8.8
0,002	2.7	1,42	74,3	16.8
0.003	10.0	2,96	106.2	23,6
0.004	23.7	5,16	129.9	28.6
0.005	22.8	5.49	137,6	30.3
0.006	15,5	4.14	126.9	28.2
0.007	8,4	2.59	104.0	23,4
0.008	4.3	1.60	74.4	16.9
0.009	1.2	0.71	39.6	9.1
0.01	0.3	0.09	1.4	0.3
0,0045	24,5	5.57	-	-

Table VI presents the final results of the analysis, which are obtained by the conversion of the corresponding values in Table V. The final, comparable plots are presented in Fig. 12.

TABLE VI

Time, sec.	Current, A			
	'O' duty		'K' duty	
	Choke A	Choke B	Choke A	Choke B
0.	0.0	0.0	0	0
0.001	1.9	6.7	83	86
0.002	5.8	13.9	160	164
0.003	21.6	29.0	230	231
0.004	51.2	50.5	281	281
0.005	49.3	53.8	297	297
0.006	33.6	40.7	274	276
0.007	18.2	25.4	224	229
0.008	9.3	15,7	160	166
0.009	2.6	7.0	85	89
0.01	0.6	0.9	3	3
0.0045	52.9	59.5	-	-

6. THE CONCLUSION

The presented analysis, performed with the method elaborated in this work, results in the approximate evaluation of the current waveforms in the two simplified welding circuits, as shown in figure 1, with the same supply voltage U_e and the same linear resistances R. The proportions of the current shape are nearly the same at the regulating range of the 300A maximum value and differ at the 50A maximum value. This diversity corresponds to the specially resolved diversity in the magnetic parameters of the reactors. These parameters are related to the inductance action form.

The curves plotted in figure 12 prove that the influence of the saturation characteristic curvature is of considerable practical importance for the evaluation of the suitability for welding of manual metal arc welding transformers. Two transformers with nearly the same Carrer's factors at the 300A

maximum current value range, appear to have entirely different factors at the 50A range.

References

1. A. CARRER: Comportamento dinamico di trasformatori per saldatura ad arco. Proposta per una definizione di attitudine alla saldatura. Riv. Ital. Saldat., 1963, vol. 15, No. 1, p. 3-28.

2. A. CARRER: Comportamento dinamico di trasformatori per saldatura ad arco. Ulteriori ricerche sperimentali. Riv. Ital. Saldat., 1963, vol. 15, No. 3, p. 137-150.

3. B.E. PATON, V.K. LEBEDEV: Elementy raschetov tsepei i apparatov peremennogo toka dlya dugovoi svarki. Kiev, 1953, Izdat. AN USSR. (p. 10-38).

4. D.D. McCRACKEN, W.S. DORN: Numerical Methods and Fortran Programming. New York, 1964. J. Wiley (p. 317-321).

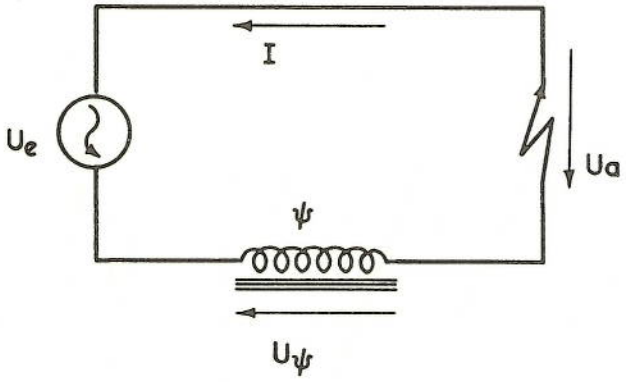

FIG. 1 THE DIAGRAM OF THE CONSIDERED CIRCUIT.

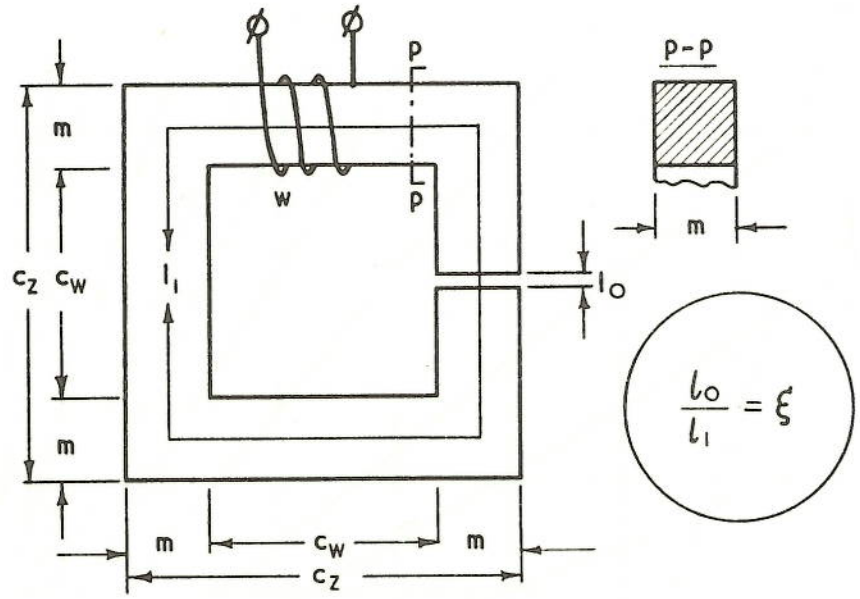

	c_w	c_z	m	w
	mm	mm	mm	—
(A)	20	34	7	50
(B)	36	62	13	20

FIG. 2 DATA OF THE RESOLVED CHOKES A AND B.

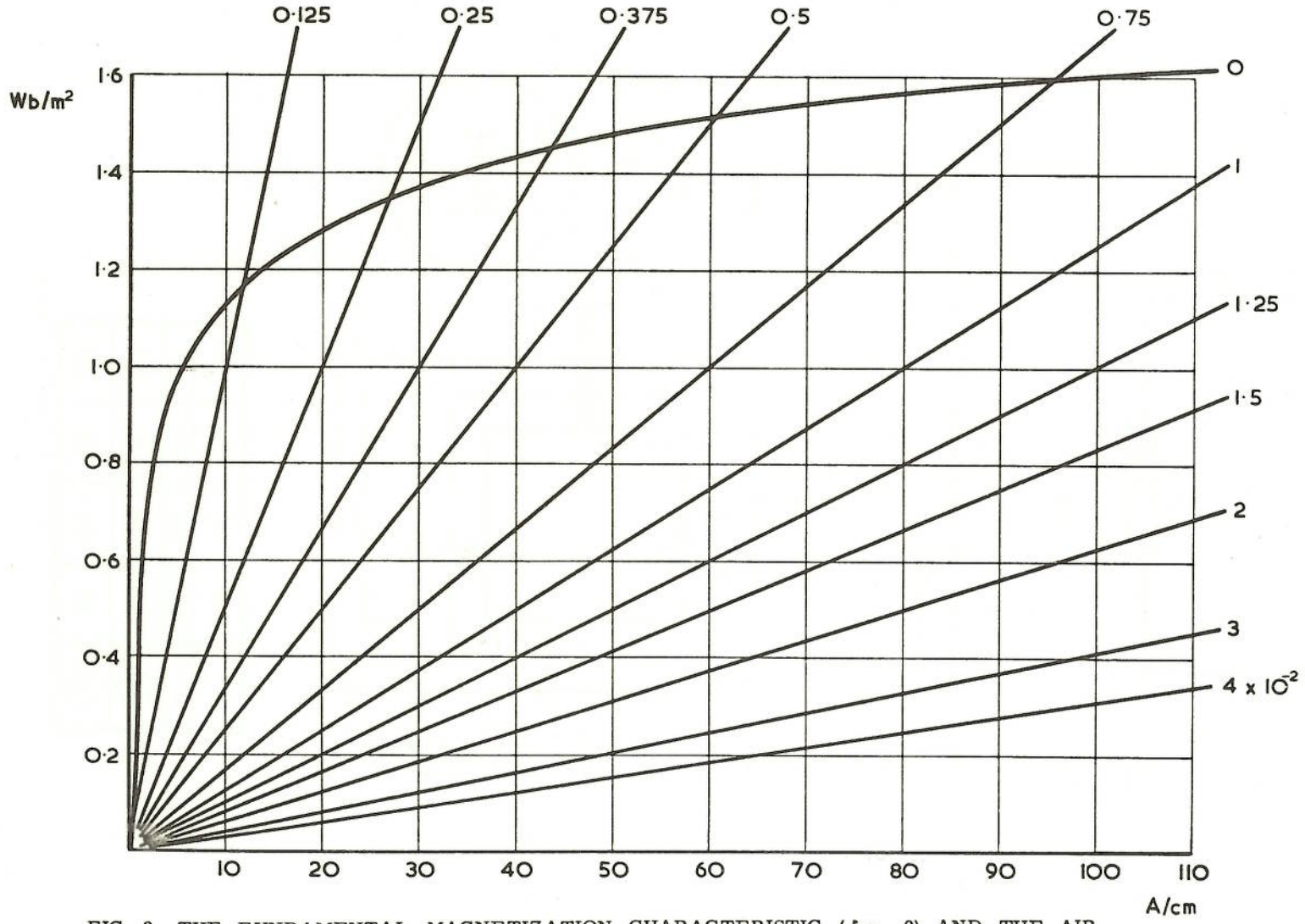

FIG. 3 THE FUNDAMENTAL MAGNETIZATION CHARACTERISTIC (ξ = 0) AND THE AIR GAP CHARACTERISTICS AT VARIOUS VALUES OF ξ.

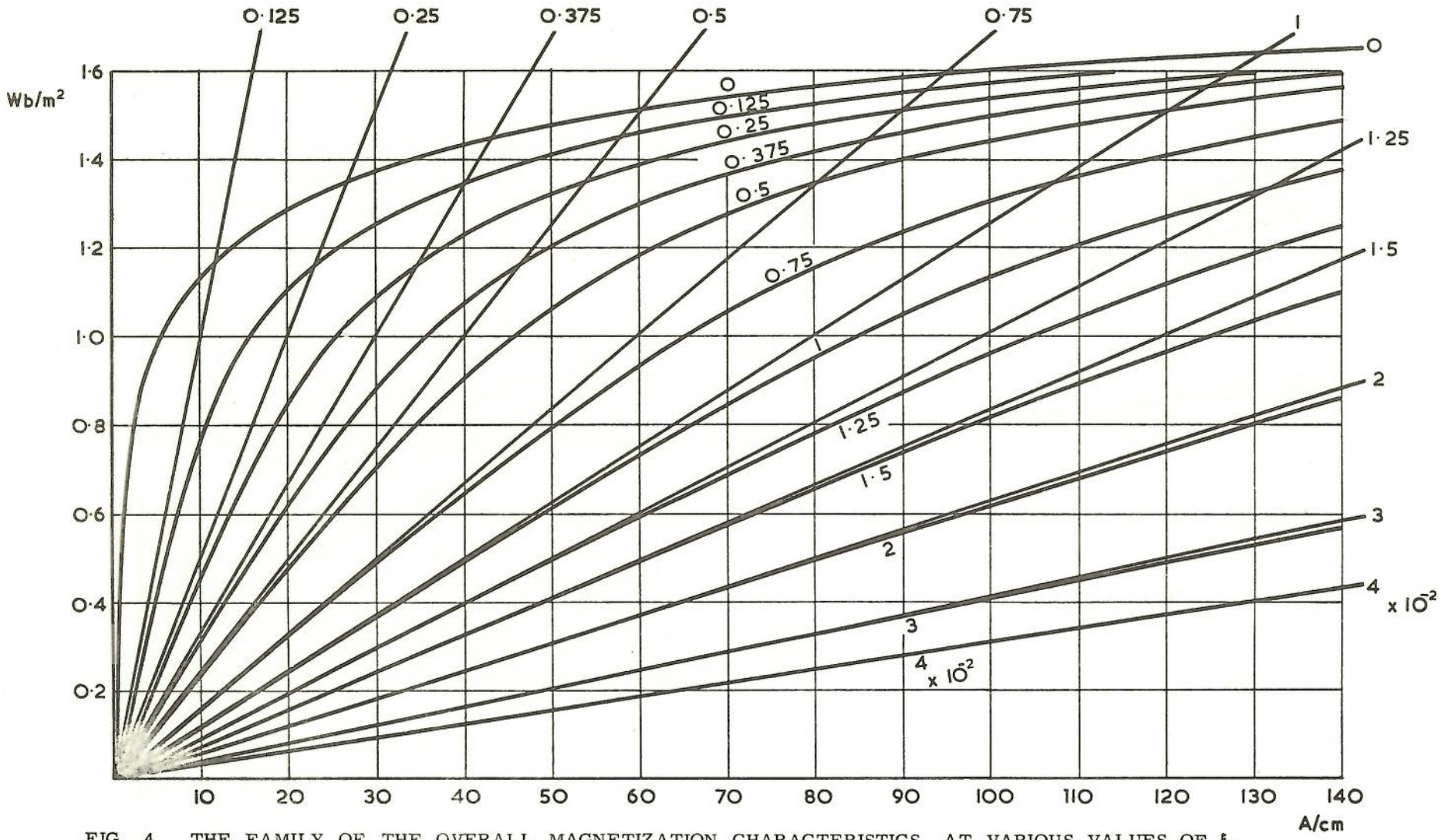

FIG. 4 THE FAMILY OF THE OVERALL MAGNETIZATION CHARACTERISTICS, AT VARIOUS VALUES OF ξ. THE OVERALL CURVES HAVE BEEN CONSTRUCTED GRAPHICALLY FROM THE FUNDAMENTAL MAGNETIZATION CURVE (ξ = 0) AND FROM THE SHOWN STRAIGHT LINES DESCRIBING THE AIR GAP CHARACTERISTICS.

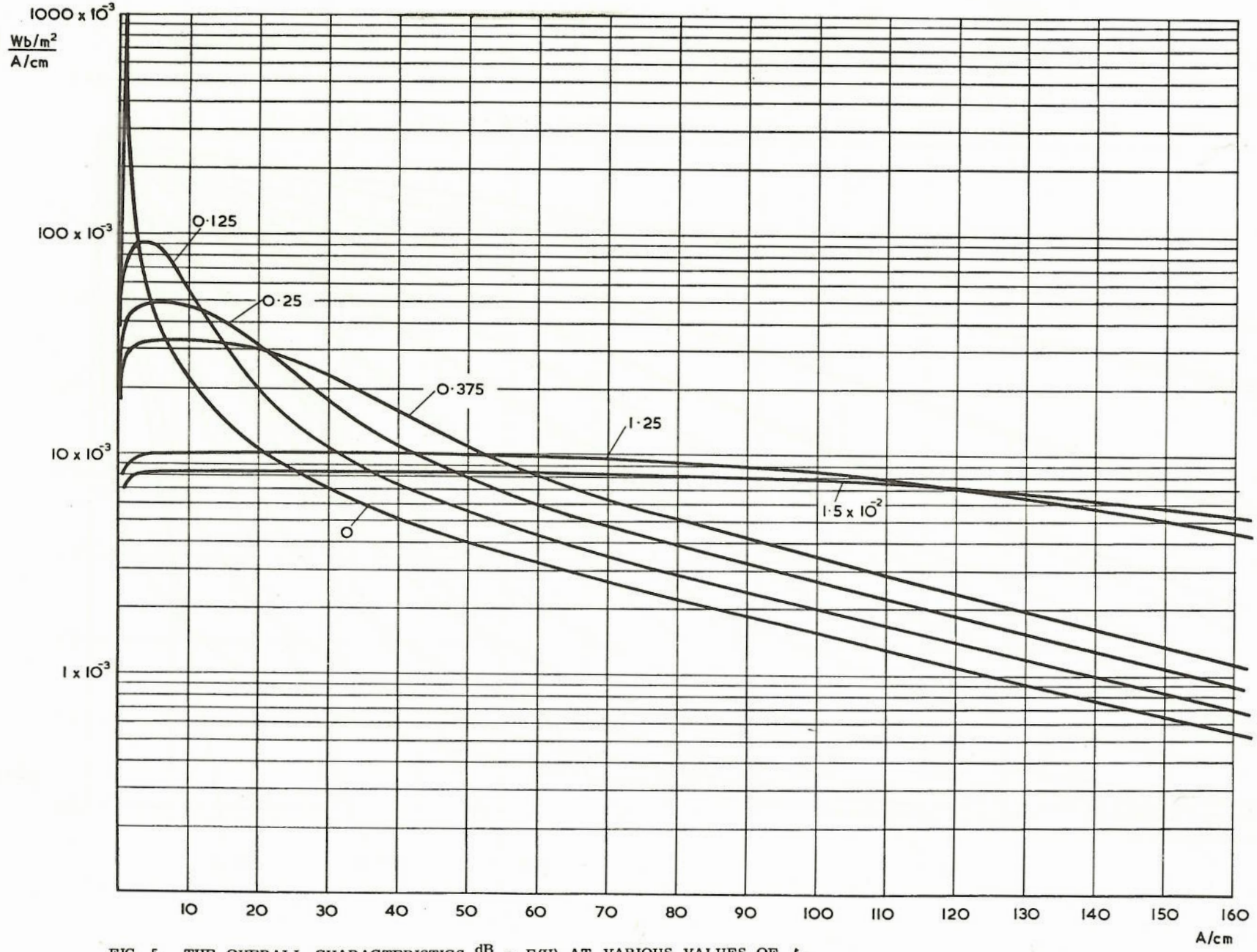

FIG. 5 THE OVERALL CHARACTERISTICS $\frac{dB}{dH}$ = F(H) AT VARIOUS VALUES OF ξ.

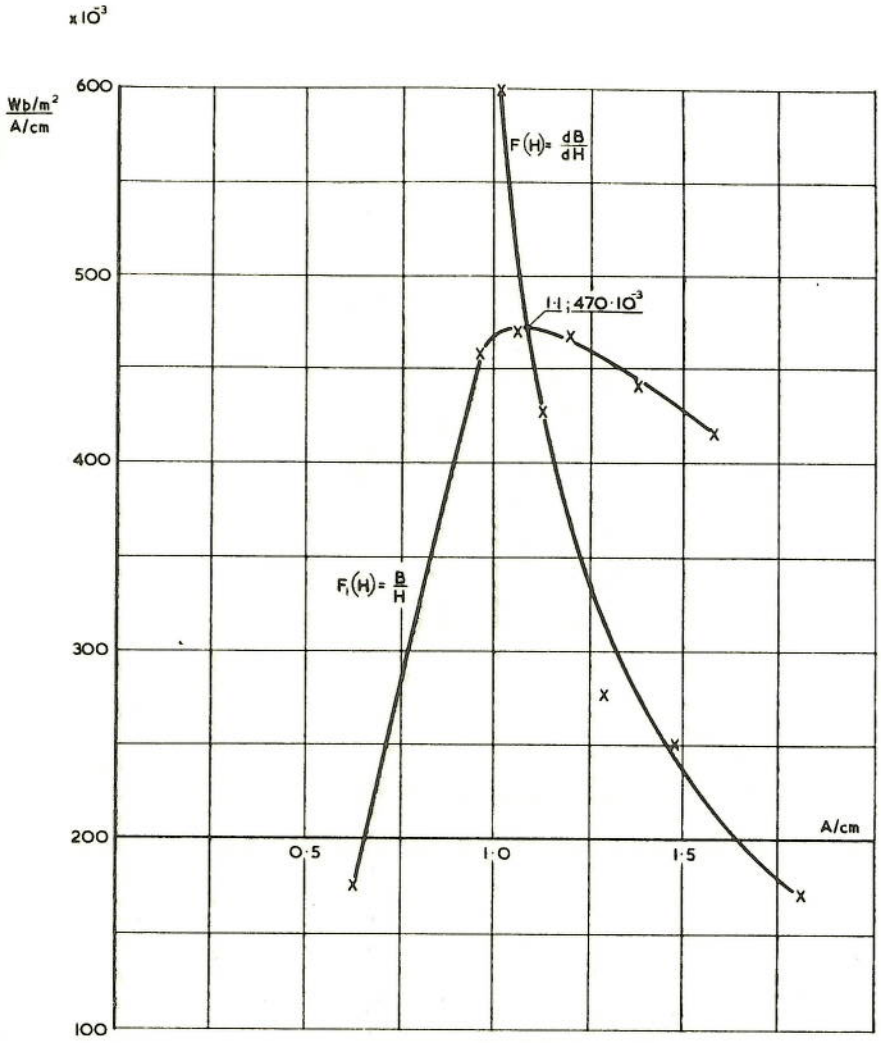

FIG. 6 THE GRAPHICAL EVALUATION OF THE POINT THAT LIMITS THE LINEAR APPROXIMATION OF THE FUNDAMENTAL MAGNETIZATION CHARACTERISTIC ($\xi = 0$). THE POINT IS RELATED TO IDENTICAL VALUES OF $\frac{dB}{dH}$ AND $\frac{B}{H}$.

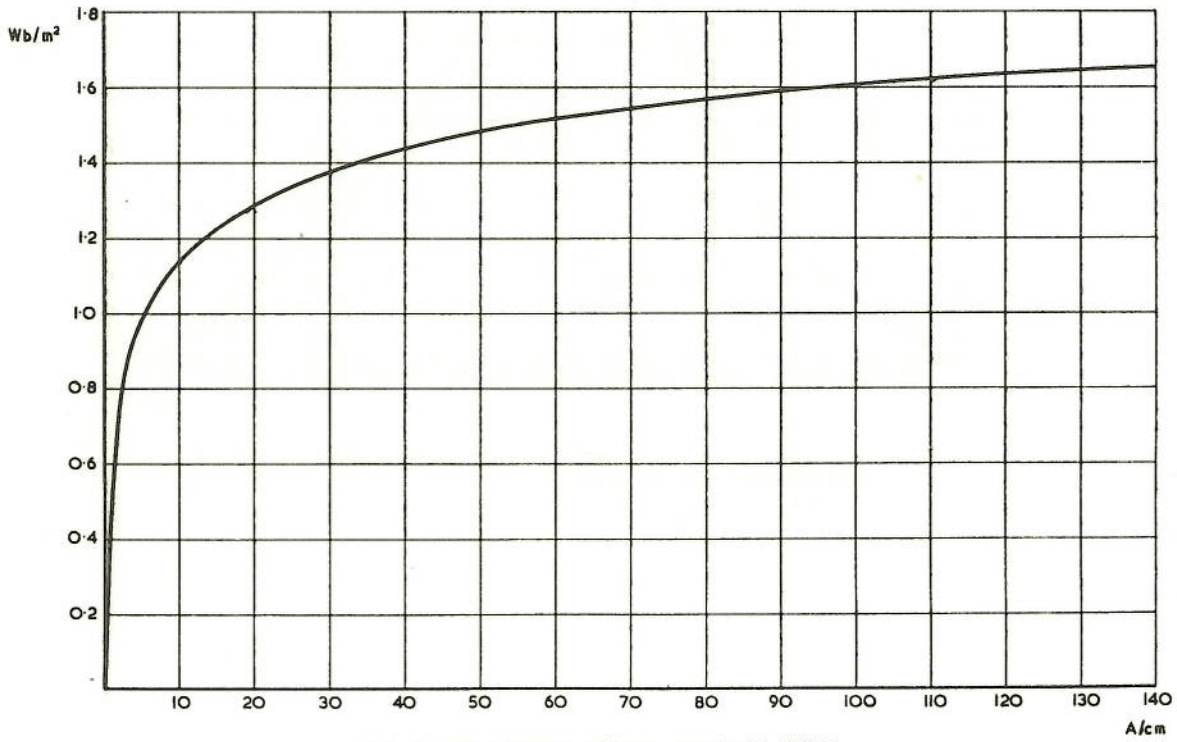

FIG. 7 THE MODIFIED NORMAL INDUCTION CURVE

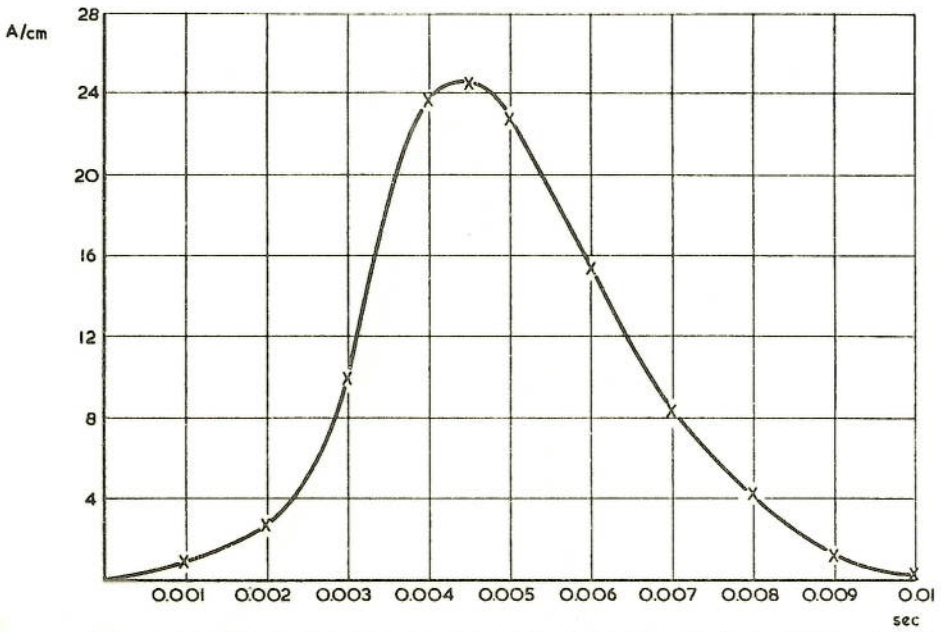

FIG. 8 THE EVALUATED WAVEFORM OF THE MAGNETIC FIELD STRENGTH IN THE CHOKE A AT "0" DUTY

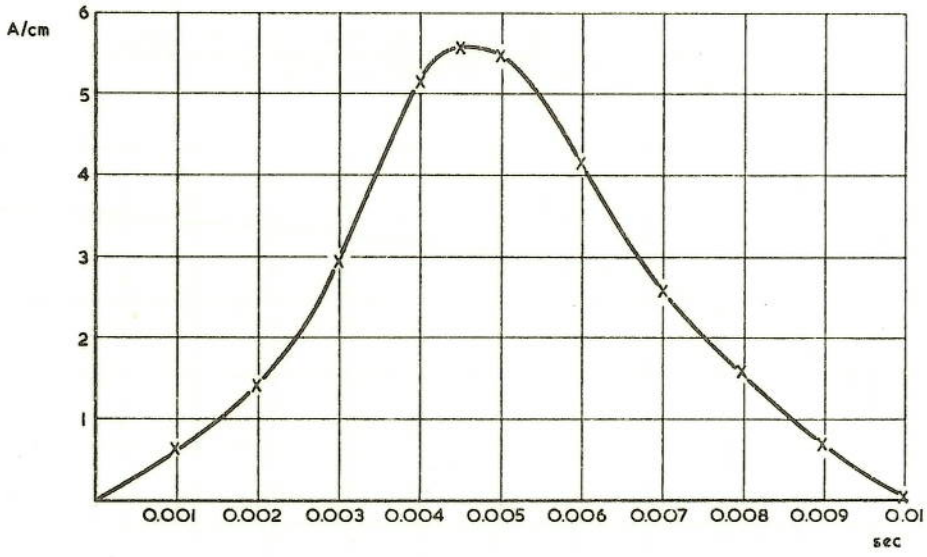

FIG. 9 THE EVALUATED WAVEFORM OF THE MAGNETIC FIELD STRENGTH IN THE CHOKE B AT "0" DUTY

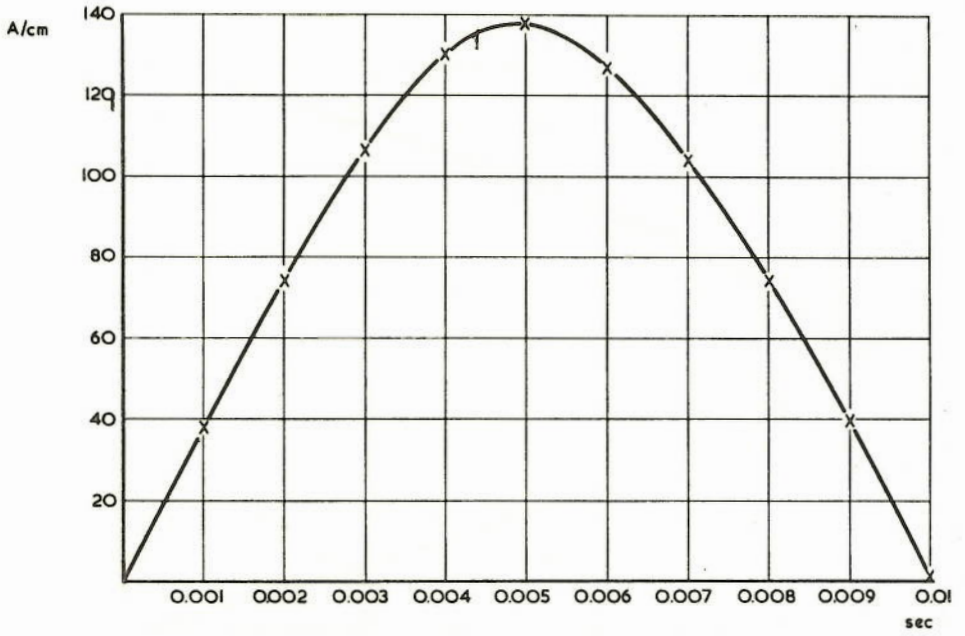

FIG. 10 THE EVALUATED WAVEFORM OF THE MAGNETIC FIELD STRENGTH IN THE CHOKE A AT "K" DUTY

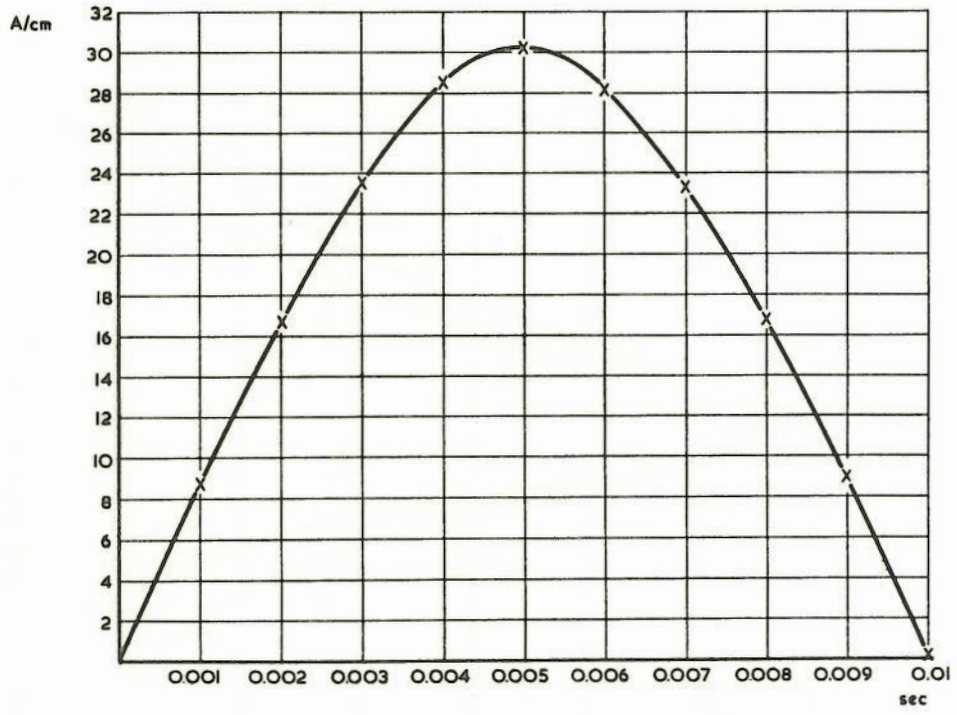

FIG. 11 THE EVALUATED WAVEFORM OF THE MAGNETIC FIELD STRENGTH IN THE CHOKE B AT "K" DUTY

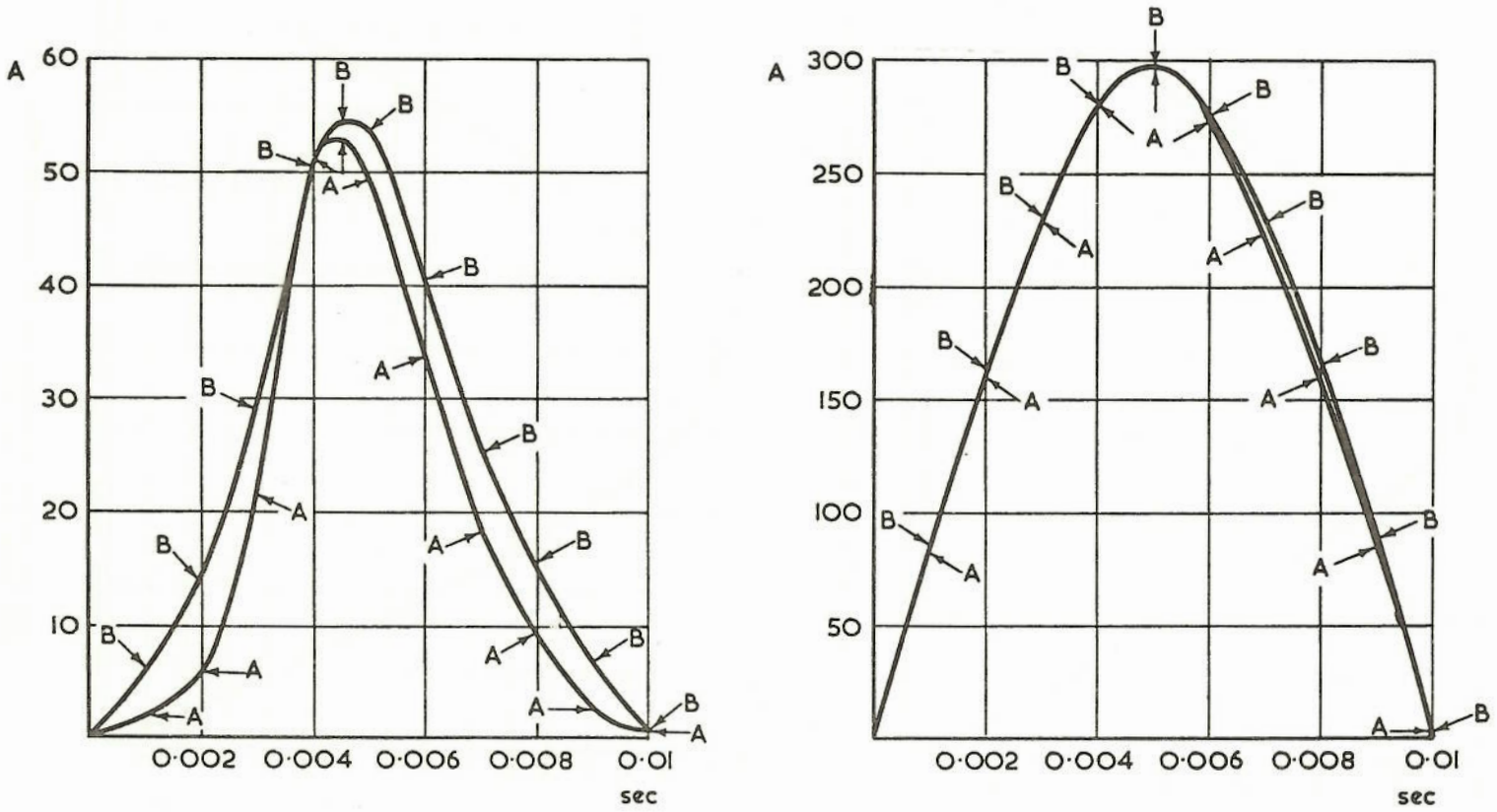

FIG. 12 THE RESULTS OF THE ANALYSIS: THE EVALUATED CURRENT WAVEFORMS. ARROWS INDICATE THE ESTIMATED POINTS (FOR CHOKES A AND B). 60A SCALE-"O" DUTY; 300A SCALE - "K" DUTY.